

# Synthesis and Characterization of Novel Triarylamine Derivatives with Dimethylamino Substituents for Application in Optoelectronic Devices

Jung-Tsu Wu,<sup>†,§</sup> Hsiang-Ting Lin,<sup>†,§</sup> and Guey-Sheng Liou<sup>\*,†,‡,§</sup>

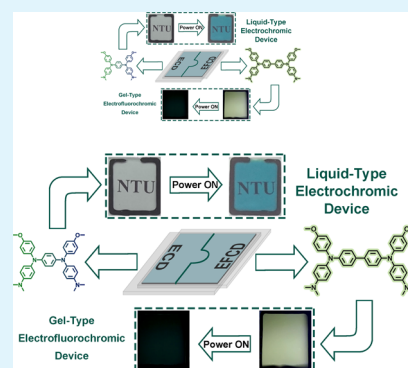
<sup>†</sup>Functional Polymeric Materials Laboratory, Institute of Polymer Science and Engineering, National Taiwan University, 1 Roosevelt Road, 4th Sec., Taipei 10617, Taiwan

<sup>‡</sup>Advanced Research Center for Green Materials Science and Technology, National Taiwan University, Taipei 10607, Taiwan

## Supporting Information

**ABSTRACT:** Two novel triphenylamine-based derivatives with dimethylamino substituents, *N,N'*-bis(4-dimethylaminophenyl)-*N,N'*-bis(4-methoxyphenyl)-1,4-phenylenediamine (NTPPA) and *N,N'*-bis(4-dimethylaminophenyl)-*N,N'*-bis(4-methoxyphenyl)-1,1'-biphenyl-4,4'-diamine (NTPB), were readily prepared for investigating the optical and electrochromic behaviors. These two obtained materials were introduced into electrochromic devices accompanied with heptyl viologen (HV), and the devices demonstrate a high average coloration efficiency of 287 cm<sup>2</sup>/C and electrochemical stability. Besides, NTPB/HV was further used to fabricate electrofluorochromic devices with a gel type electrolyte, and exhibit a controllable and high photoluminescence contrast ratio ( $I_{\text{off}}/I_{\text{on}}$ ) of 32.12 from strong emission to truly dark by tuning the applied potential in addition to a short switching time of 4.9 s and high reversibility of 99% after 500 cycles.

**KEYWORDS:** electrochromism, electrofluorochromism, ambipolar, triphenylamine, dimethylamino



## INTRODUCTION

In 1961, Platt reported an interesting phenomenon of electrochromism that the color of materials could be tuned or changed reversibly by gaining or losing electrons during the electrochemical process.<sup>1</sup> Then, various electrochromic (EC) materials have been reported and widely applied in our daily life,<sup>2–4</sup> for example, color-changing windows in Boeing 787 Dreamliner and night vision safety mirror products by Gentex. These EC materials can be simply classified into inorganic and organic categories.<sup>5–11</sup> Inorganic materials have been investigated since Deb published the first paper by using EC tungsten oxide in 1969.<sup>12</sup> Compared to inorganic type materials, organic EC materials can be fabricated into devices with an easier process and lower cost.<sup>13</sup>

Based on the concept of electrochromism, researchers started to combine it with fluorescence. In the 1990s, some electrochemically monitored fluorescent materials and devices started to pop up.<sup>14</sup> The phenomenon of “electrofluorochromism” was mentioned by Rusalov et al. in 2004,<sup>15</sup> and the first electrofluorochromic (EFC) device was fabricated by Kim et al.<sup>16</sup> Then, many research groups began to focus on this interesting area.<sup>17–20</sup>

In 2017, Xu et al. published a material with a structure of oxadiazole and thiophene units which can turn from the emitting neutral state into the non-emitting oxidation state.<sup>21</sup> Then, Malik et al. electropolymerized a triphenylamine (TPA) end-capped dendron with an EC optical contrast of 68% and

EFC photoluminescence (PL) contrast ratio of 179 during the oxidation switching process.<sup>22</sup> Meanwhile, a gel-type EFC device derived from TPA-containing polyamide has also been fabricated by our group and Tang, which demonstrates a short EFC switching time of <4.9 s.<sup>23</sup> TPA-based materials are well-known for optoelectronic applications due to the excellent electron-donating nature, easy oxidizability, and hole-transporting ability.<sup>24–26</sup> TPA-containing polymers are easy to acquire high EC performance of optical contrast ratio by tuning the film thickness. However, the response time for switching on and bleaching off would be increased;<sup>27</sup> on the contrary, small molecular materials can effectively avoid such kind of sacrifice.<sup>28,29</sup>

Dimethylamino moieties are often incorporated into the anodic EC materials because of the stronger electron-donating ability than the methoxy group. The simplest and most popular material containing dimethylamino groups is *N,N,N',N'*-tetramethyl-1,4-phenylenediamine which has already been investigated in display applications for a long time.<sup>30,31</sup> In 2008, we have also successfully introduced such a group into a TPA-containing polymer system.<sup>32</sup>

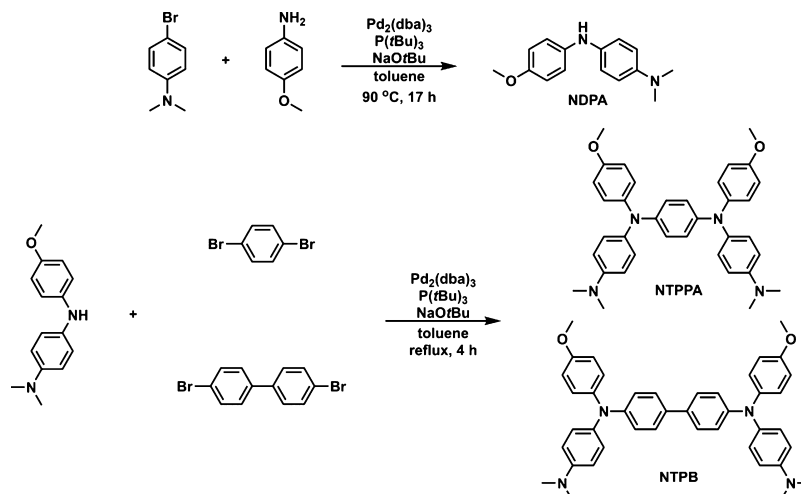
Herein, two novel TPA-based derivatives, *N,N'*-bis(4-dimethylaminophenyl)-*N,N'*-bis(4-methoxyphenyl)-1,4-phenylenediamine (NTPPA) and *N,N'*-bis(4-dimethylaminophenyl)-*N,N'*-bis(4-methoxyphenyl)-1,1'-biphenyl-4,4'-diamine (NTPB) were synthesized and characterized.

**Received:** January 8, 2019

**Accepted:** March 29, 2019

**Published:** March 29, 2019

Scheme 1. Synthesis Routes of the Materials



nylenediamine (NTPPA) and *N,N'*-bis(4-dimethylaminophenyl)-*N,N'*-bis(4-methoxyphenyl)-1,1'-biphenyl-4,4'-diamine (NTPB), were prepared in this work and were used to fabricate the electrochromic devices (ECDs) with heptyl viologen (HV). The obtained devices demonstrate a short switching time, high coloration efficiency, and good electrochemical stability. Furthermore, NTPB was further incorporated into a gel type EFC device that could control the fluorescence intensity from an intense emission to truly quench dark state with a short response time and excellent reversibility.

## EXPERIMENTAL SECTION

**Monomer Synthesis.** *N,N*-Dimethyl-*N'*-(4-methoxyphenyl)-1,4-phenylenediamine (NDPA). Tris(dibenzylideneacetone)dipalladium(0) ( $\text{Pd}_2(\text{dba})_3$ , 0.27 g, 0.30 mmol) and tri-*tert*-butylphosphine ( $\text{P}(\text{tBu})_3$ , 0.14 mL, 0.59 mmol) were added to a reactor containing 60 mL anhydrous toluene under a nitrogen atmosphere with stirring at room temperature for 10 min to undergo a ligand exchange, then *p*-anisidine (2.02 g, 16.5 mmol) was added to the flask sequentially and stirred at 50 °C till the *p*-anisidine dissolved completely. 4-Bromo-*N,N*-dimethylaniline (3.00 g, 15.0 mmol) and sodium *tert*-butoxide ( $\text{NaOtBu}$ , 11.00 g, 0.11 mol) were added to the solution, and the mixture was stirred at 90 °C for 15 h, then extracted with ethyl acetate and water till the water layer was cleared. The organic layer was dried over  $\text{MgSO}_4$  and a rotary evaporator. The residue was purified by flash column and recrystallized from hexane to obtain 1.96 g of pale orange crystal (54% yield), mp 78–79 °C. FT-IR (KBr)  $\nu$ : 3413, 3282, 3035, 2952, 2881, 2834, 2800, 1617, 1513, 1308, 1236, 1037, 813;  $^1\text{H}$  NMR (400 MHz,  $\text{DMSO}-d_6$ ,  $\delta$ ): 7.28 (s, 1H,  $\text{H}_d$ ), 6.90–6.84 (m, 4H,  $\text{H}_{b+c}$ ), 6.78–6.76 (d, 2H,  $\text{H}_e$ ), 6.69–6.67 (d, 2H,  $\text{H}_f$ ), 3.66 (s, 3H,  $\text{H}_a$ ), 2.79 (s, 6H,  $\text{H}_g$ ).

*N,N'*-Bis(4-dimethylaminophenyl)-*N,N'*-bis(4-methoxyphenyl)-1,4-phenylenediamine (NTPPA). Palladium(II) acetate ( $\text{Pd}(\text{OAc})_2$ , 36 mg, 0.16 mmol) and  $\text{P}(\text{tBu})_3$  (0.036 mL, 0.13 mmol) were added to a 50 mL reactor containing 10 mL anhydrous toluene. NDPA (1.53 g, 6.30 mmol), 1,4-dibromobenzene (0.708 g, 3.00 mmol), and  $\text{NaOtBu}$  (0.96 g, 10.0 mmol) were added to the flask sequentially, and the mixture was refluxed for 4 h. Then, the mixture was precipitated into methanol after cooling to room temperature and purified by flash column to obtain 1.04 g of yellow powder (62% yield), mp 201–203 °C (measured by DSC with a scan rate of 5 °C/min). FT-IR (KBr)  $\nu$ : 3037, 2947, 2832, 2796, 1610, 1504, 1239, 1037, 820;  $^1\text{H}$  NMR (400 MHz,  $\text{DMSO}-d_6$ ,  $\delta$ ): 6.90–6.87 (q, 8H,  $\text{H}_{b+e}$ ), 6.83–6.81 (d, 4H,  $\text{H}_c$ ), 6.70–6.67 (t, 8H,  $\text{H}_{d+f}$ ), 3.70 (s, 6H,  $\text{H}_a$ ), 2.84 (s, 12H,  $\text{H}_g$ );  $^{13}\text{C}$  NMR (100 MHz,  $\text{DMSO}-d_6$ ,  $\delta$ ): 154.4 ( $\text{C}_2$ ), 146.9 ( $\text{C}_{11}$ ), 142.1 ( $\text{C}_5$ ), 141.3 ( $\text{C}_6$ ), 137.1 ( $\text{C}_8$ ), 125.9 ( $\text{C}_9$ ), 124.3 ( $\text{C}_3$ ), 122.1 ( $\text{C}_7$ ), 114.6 ( $\text{C}_4$ ), 113.6 ( $\text{C}_{10}$ ), 55.2 ( $\text{C}_1$ ), 40.5 ( $\text{C}_{12}$ ); MS (ESI)  $m/z$ :  $[\text{M} + \text{H}]^+$

calcd for  $\text{C}_{36}\text{H}_{38}\text{N}_4\text{O}_2$ , 558.30; found, 558.30. Anal. Calcd for  $\text{C}_{36}\text{H}_{38}\text{N}_4\text{O}_2$ : C, 77.39; H, 6.86; N, 10.03. Found: C, 76.94; H, 6.86; N, 9.88.

*N,N'*-Bis(4-dimethylaminophenyl)-*N,N'*-bis(4-methoxyphenyl)-1,1'-biphenyl-4,4'-diamine (NTPB).  $\text{Pd}(\text{OAc})_2$  (36 mg, 0.16 mmol) and  $\text{P}(\text{tBu})_3$  (0.036 mL, 0.13 mmol) were added to a 50 mL flask containing 10 mL anhydrous toluene. NDPA (1.53 g, 6.30 mmol), 4,4'-dibromo-1,1'-biphenyl (0.939 g, 3.00 mmol), and  $\text{NaOtBu}$  (0.960 g, 10.0 mmol) were added to the container sequentially, and the solution was refluxed for 4 h. Then, the mixture was precipitated into methanol after cooling to room temperature and purified by flash column to obtain 1.54 g of light yellow powder (81% yield), mp 197–201 °C (measured by DSC with a scan rate of 5 °C/min). FT-IR (KBr)  $\nu$ : 3033, 2930, 2832, 2797, 1615, 1505, 1492, 1240, 1036, 817;  $^1\text{H}$  NMR (400 MHz,  $\text{DMSO}-d_6$ ,  $\delta$ ): 7.37–7.35 (d, 4H,  $\text{H}_c$ ), 7.01–7.00 (d, 4H,  $\text{H}_b$ ), 6.96–6.94 (d, 4H,  $\text{H}_f$ ), 6.89–6.88 (d, 4H,  $\text{H}_e$ ), 6.78–6.76 (d, 4H,  $\text{H}_d$ ), 6.73–6.71 (d, 4H,  $\text{H}_g$ ), 3.73 (s, 6H,  $\text{H}_a$ ), 2.87 (s, 12H,  $\text{H}_h$ );  $^{13}\text{C}$  NMR (100 MHz,  $\text{DMSO}-d_6$ ,  $\delta$ ): 155.3 ( $\text{C}_2$ ), 147.5 ( $\text{C}_{13}$ ), 147.3 ( $\text{C}_6$ ), 140.4 ( $\text{C}_5$ ), 136.2 ( $\text{C}_{10}$ ), 131.2 ( $\text{C}_9$ ), 126.9 ( $\text{C}_{11}$ ), 126.4 ( $\text{C}_8$ ), 126.0 ( $\text{C}_3$ ), 119.2 ( $\text{C}_7$ ), 114.8 ( $\text{C}_4$ ), 113.6 ( $\text{C}_{12}$ ), 55.2 ( $\text{C}_1$ ), 40.4 ( $\text{C}_{14}$ ); MS (ESI)  $m/z$ :  $[\text{M} + \text{H}]^+$  calcd for  $\text{C}_{42}\text{H}_{42}\text{N}_4\text{O}_2$ , 634.33; found, 634.33. Anal. Calcd for  $\text{C}_{42}\text{H}_{42}\text{N}_4\text{O}_2$ : C, 79.46; H, 6.67; N, 8.83. Found: C, 78.90; H, 6.90; N, 8.89.

## RESULTS AND DISCUSSION

### Synthesis and Basic Characterization of Materials.

*N,N*-Dimethyl-*N'*-(4-methoxyphenyl)-1,4-phenylenediamine (NDPA) was first synthesized by using Buchwald–Hartwig amination with a yield of 54% from *p*-anisidine and 4-bromo-*N,N*-dimethylaniline.<sup>6</sup> NDPA was further reacted with 1,4-dibromobenzene and 4,4'-dibromo-1,1'-biphenyl, respectively, to obtain two new compounds, *N,N'*-bis(4-dimethylaminophenyl)-*N,N'*-bis(4-methoxyphenyl)-1,4-phenylenediamine (NTPPA), and *N,N'*-bis(4-dimethylaminophenyl)-*N,N'*-bis(4-methoxyphenyl)-1,1'-biphenyl-4,4'-diamine (NTPB) with a yield of 62 and 81%. The synthetic routes are summarized in Scheme 1. The structures of these two new compounds were first compared with NDPA by using Fourier transform infrared (FT-IR) as shown in Figures S1 and S2. According to the spectra, the peaks at the range of 3000–2700  $\text{cm}^{-1}$  belong to the C–H stretching, while the N–H stretching of NDPA in the range of 3470–3130  $\text{cm}^{-1}$  disappeared for NTPPA and NTPB. The more detail confirmation of the structures was demonstrated by the NMR measurement, and the results are depicted in Figures S3–S11.

**Optical and EC Behaviors.** The UV–vis absorption and PL behaviors of these materials were investigated in a dilute solution (10  $\mu\text{M}$ ) of dimethyl sulfoxide (DMSO) and solid state at room temperature, and the results are listed in Table 1.

**Table 1. Optical Properties of TPA-Based Materials**

	solution			powder		
	$\lambda_{\text{max}}^{\text{abs}}$ [nm]	$\lambda_{\text{max}}^{\text{em}}$ [nm] <sup>a</sup>	$\Phi_{\text{PL}}^{\text{sol}}$ [%] <sup>b</sup>	$\lambda_{\text{max}}^{\text{abs}}$ [nm]	$\lambda_{\text{max}}^{\text{em}}$ [nm] <sup>a</sup>	$\Phi_{\text{PL}}^{\text{solid}}$ [%] <sup>c</sup>
NTPPA	316	442	2.6	332	458	2.2
NTPB	360	471	1.7	379	477	29.5

<sup>a</sup>Both of  $\lambda_{\text{max}}^{\text{em}}$  were excited at  $\lambda_{\text{max}}^{\text{abs}}$ . <sup>b</sup>The quantum yield was measured by using quinine sulfate as a standard at 25 °C (concentration of 10  $\mu\text{M}$  in 1 N H<sub>2</sub>SO<sub>4</sub>, assuming a PL quantum efficiency of 0.546). <sup>c</sup>PL quantum yields of solid-state molecules were determined by using a calibrated integrating sphere.

Both NTPPA and NTPB reveal absorption bands at 316 and 360 nm in DMSO solution as shown in Figure 1a, and the

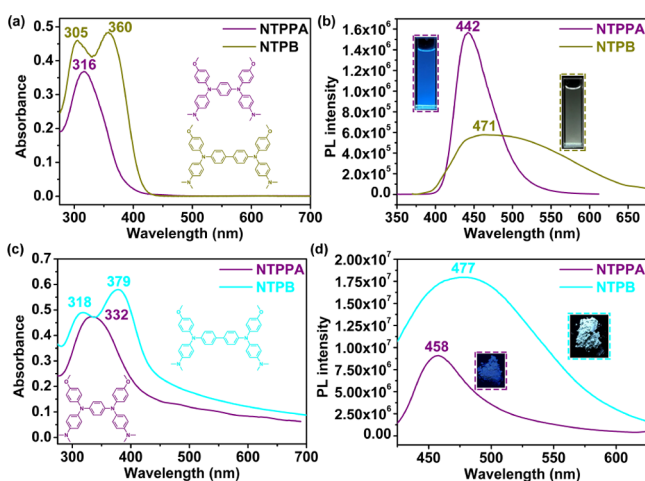


**Figure 1.** (a) Absorption spectra of NTPPA and NTPB in DMSO solution. (b) PL spectra of NTPPA and NTPB in DMSO solution. (Solution concentration: 10  $\mu\text{M}$ ) (c) Absorption spectra of NTPPA and NTPB in the solid state. (d) PL spectra of NTPPA and NTPB in the solid state.

corresponding PL spectra display maximum bands at 442 and 471 nm as shown in Figure 1b, respectively. Figure 1c,d exhibit the UV–vis absorption and PL spectra of the same materials in the solid state, showing absorption peaks at 332 and 379 nm, and PL emission peaks at 458 and 477 nm, respectively.

Based on the results depicted in Figure 1 and Table 1, NTPB demonstrates an AIE property with an  $\alpha_{\text{AIE}}$  of 17.4 calculated from the quantum yield in the solid state of 29.5% and DMSO solution of 1.7%. According to the single crystal packing diagrams illustrated in Figure 2, NTPPA containing three molecules in every unit cell possesses several CH/ $\pi$  interactions with each other with a distance from 2.796 to 3.395 Å, while NTPB shows CH/ $\pi$  interactions only between every two molecules with a distance from 2.804 to 3.335 Å. Consequently, the energy of NTPPA can transfer between every three molecules but NTPB can only transfer between every two molecules, resulting in lower quantum yield for NTPPA in the solid state.

The electrochemical behavior of these two novel EC materials was investigated by differential pulse voltammetry

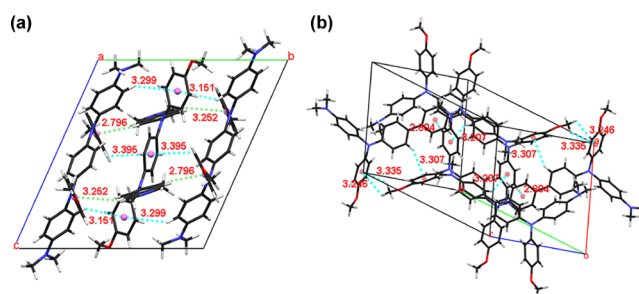


**Figure 2.** Single crystal packing diagrams and CH/ $\pi$  interaction of (a) NTPPA and (b) NTPB in a unit cell.

(DPV) using a quartz cell with a platinum net as the working electrode in anhydrous GBL containing 1 mM EC materials and 0.1 M TBABF<sub>4</sub> as the supporting electrolyte under the nitrogen atmosphere for oxidation measurements, respectively. Figure 3a,b depict the DPV diagrams of the obtained EC

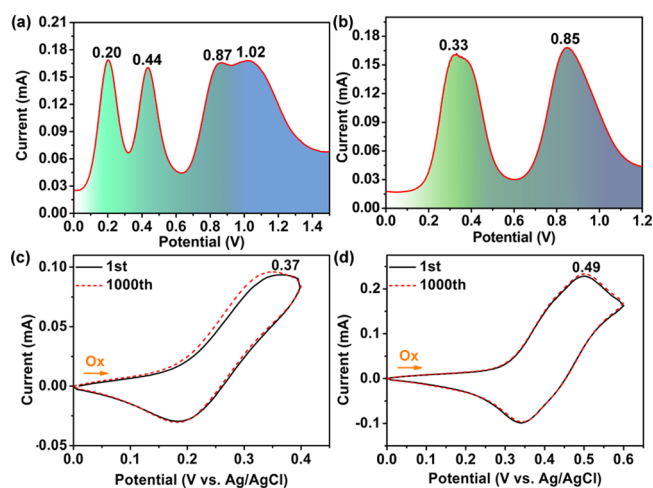


**Figure 3.** Differential pulse voltammograms of (a) NTPPA and (b) NTPB conducted with a platinum net in 0.1 M tetra-*n*-butylammonium tetrafluoroborate (TBABF<sub>4</sub>)/ $\gamma$ -butyrolactone (GBL) at a scan rate of 2 mV/s, pulse width of 25 ms, pulse period of 0.2 s, and pulse amplitude of 50 mV. Continuous cyclic voltammograms of (c) NTPPA and (d) NTPB conducted with ITO-coated glass in 0.1 M TBABF<sub>4</sub> at a scan rate of 50 mV/s. (Materials concentration:  $1.0 \times 10^{-3}$  M).

materials. NTPPA showed four oxidation peaks at 0.20, 0.44, 0.87, and 1.02 V, corresponding to the number of electroactive nitrogen centers, while only two main oxidation peaks for NTPB could be observed at 0.33 and 0.85 V ascribed to the other two oxidation stages were embedded into the main peaks due to too similar potentials to be distinguished. In addition, both of the EC materials reveal excellent electrochemical stability confirmed by cyclic voltammetry (CV) with 1000 continuous cycles scanning at their first oxidation state as depicted in Figure 3c,d, respectively.

**Spectroelectrochemistry.** The spectroelectrochemical measurement was used to demonstrate EC characteristics of these materials by using an optically transparent thin-layer electrode coupled with UV–vis spectroscopy. The typical absorption spectra and the corresponding EC coloring behaviors of NTPPA and NTPB are shown in Figures 4 and 5. As shown in Figure 4a, three new characteristic absorption peaks at 421, 744, and 1079 nm appear simultaneously for

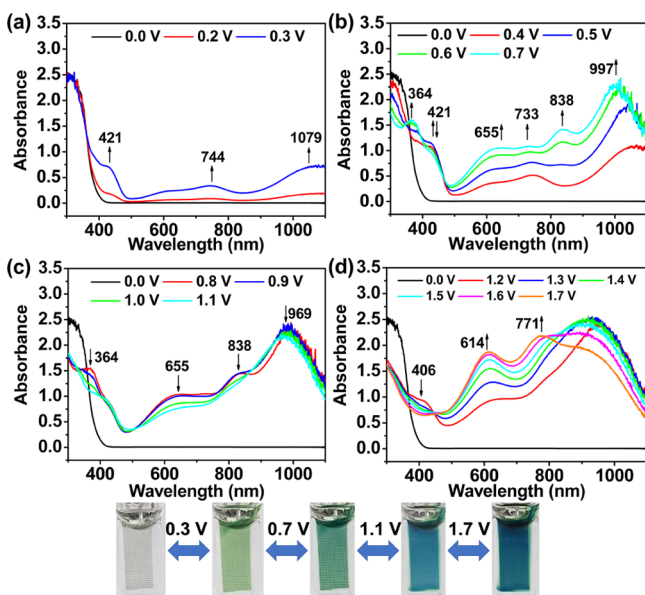


**Figure 4.** (a) Absorbance spectra for the first electron oxidation of NTPPA at the applied potential from 0.2 to 0.3 V, (b) for the second electron oxidation of NTPPA at the applied potential from 0.4 to 0.7 V, (c) for the third electron oxidation of NTPPA at the applied potential from 0.8 to 1.1 V, and (d) for the fourth electron oxidation of NTPPA at the applied potential from 1.2 to 1.7 V. NTPPA (1 mM) was dissolved in 0.1 M TBABF<sub>4</sub>/PC.

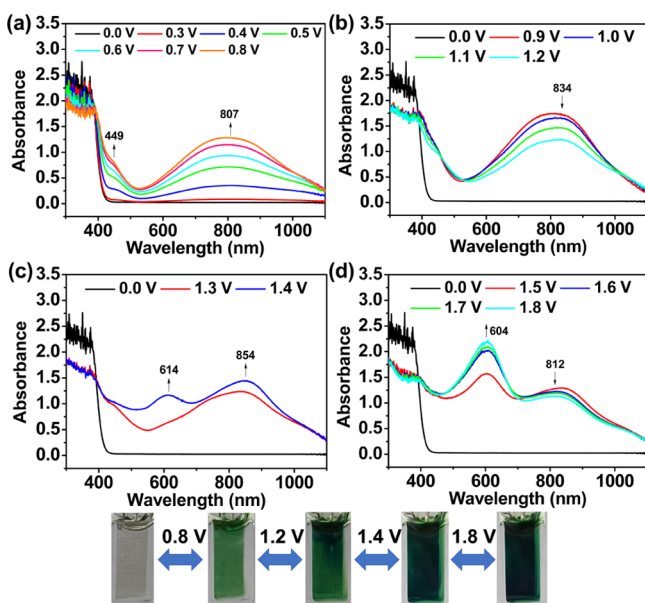


**Figure 5.** (a) Absorbance spectra for the first electron oxidation of NTPB at the applied potential from 0.0 to 0.8 V, (b) for the second electron oxidation of NTPB at the applied potential from 0.9 to 1.2 V, (c) for the third electron oxidation of NTPB at the applied potential from 1.3 to 1.4 V, and (d) for the fourth electron oxidation of NTPB at the applied potential from 1.5 to 1.8 V. NTPB (1 mM) was dissolved in 0.1 M TBABF<sub>4</sub>/PC.

NTPPA during oxidation at 0.0–0.3 V. The absorption at the near-IR region could be ascribed to the inter-valence charge transfer (IV-CT) excitation caused by the electron coupling between neutral nitrogen and cation radical nitrogen centers via the phenyl bridge.<sup>25,26</sup> When a higher potential (0.4–0.7 V) was applied to the second oxidation state, the intensity of the

characteristic absorbance peak in the UV region started to decrease, while the intensity of peaks at 744 nm and IV-CT band increases and shifts to 733 and 997 nm, respectively. Besides, three new peaks emerge at 364, 655, and 838 nm as shown in Figure 4b. The third oxidation of the NTPPA (0.8–1.1 V, Figure 4c) displays no obvious absorption change. For the last oxidation state of NTPPA as depicted in Figure 4d, two new peaks arise at 614 and 771 nm with higher absorbance. The color of NTPPA could be tuned from green to blue by gradually increasing the applied potential. For NTPB, the characteristic absorption peaks at 449 and 807 nm show up gradually during the formation of the first cationic radical state (0.0–0.8 V) as shown in Figure 5a. When applied potential increased to 0.9–1.2 V for the second oxidation state, the broadband at 807 nm decreased and shifted to 834 nm as depicted in Figure 5b. For the third oxidation state of NTPB shown in Figure 5c, two new peaks at 614 and 854 nm appeared, then the peak at 614 nm shifted to 604 nm with enhanced absorbance, while the peak at 854 nm decreased and shifted to 812 nm in the fourth oxidation state (Figure 5d).

**Electrochemical and EC Behaviors of the ECDs.** The electrochemical properties of the ambipolar liquid-type ECDs derived from NTPPA/HV and NTPB/HV in anhydrous GBL were investigated by CV, respectively. The first oxidation state was chosen for further studies, and the oxidation peaks at 0.71 and 0.92 V for NTPPA/HV and NTPB/HV are shown in Figure 6a,b. Furthermore, a spectroelectrochemical study of

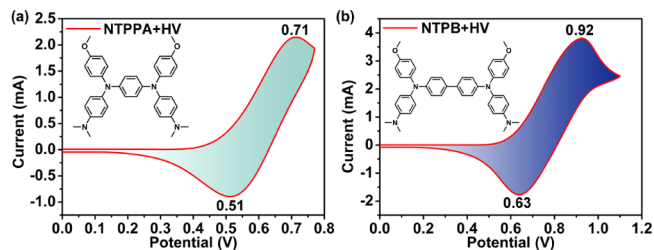


**Figure 6.** Cyclic voltammograms of the ECDs derived from (a) NTPPA/HV and (b) NTPB/HV at a scan rate of 50 mV/s. The device is ITO glass with 2 × 2 cm<sup>2</sup> active area containing 0.015/0.015 M NTPPA/HV or NTPB/HV in about 0.05 mL of GBL.

these ambipolar ECDs based on NTPPA/HV and NTPB/HV was also conducted. The typical UV–vis absorption spectra and the corresponding EC coloring behaviors for the first oxidation state of NTPPA/HV and NTPB/HV are shown in Figure 7. The change of the absorption spectra for NTPPA/HV at different working potentials from 0.0 to 0.8 V shown in Figure 7a reveals three absorption peaks (424, 606, and 738 nm) in the visible light region and one in the near-IR region. The color changed from colorless ( $L^*$ : 92.62,  $a^*$ : −5.55,  $b^*$ : 5.55) to a pale blue color ( $L^*$ : 65.42,  $a^*$ : −31.76,  $b^*$ : −2.12) with a reversibility of 99.9%. For the device of NTPB/HV, when the applied potential was given from 0.0 to 1.0 V, two peaks in the visible light region (449 and 606 nm) and one in the near-IR region appeared as shown in Figure 7b, with the color changing from colorless ( $L^*$ : 91.99,  $a^*$ : −6.54,  $b^*$ : 8.72) to a dark blue-green color ( $L^*$ : 43.95,  $a^*$ : −34.68,  $b^*$ : −12.63) and 99.9% reversibility.

**EC Switching and Stability of the ECDs.** The EC switching study of the obtained ECDs could be applied for recording the difference of the optical transmittance as a function of time and calculating the response time by stepping

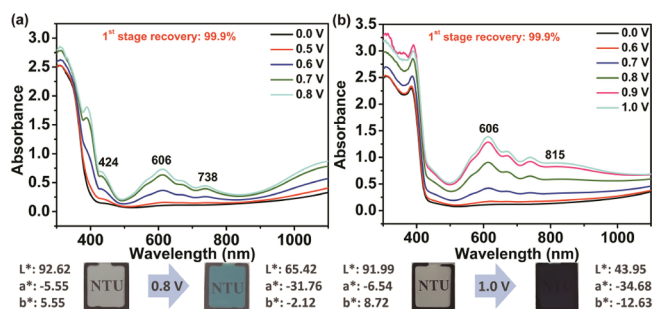


**Figure 7.** Absorbance spectra and the corresponding electrochromism of the ECD derived from (a) NTPPA/HV at the applied potential from 0.0 to 0.8 V and (b) NTPB/HV at the applied potential from 0.0 to 1.0 V. The device is ITO glass with  $2 \times 2 \text{ cm}^2$  active area containing 0.015/0.015 M NTPPA/HV or NTPB/HV in about 0.05 mL of GBL.

the potential between the bleaching and coloring states repeatedly. Switching data of the devices based on the corresponding materials are summarized in Figures 8 and

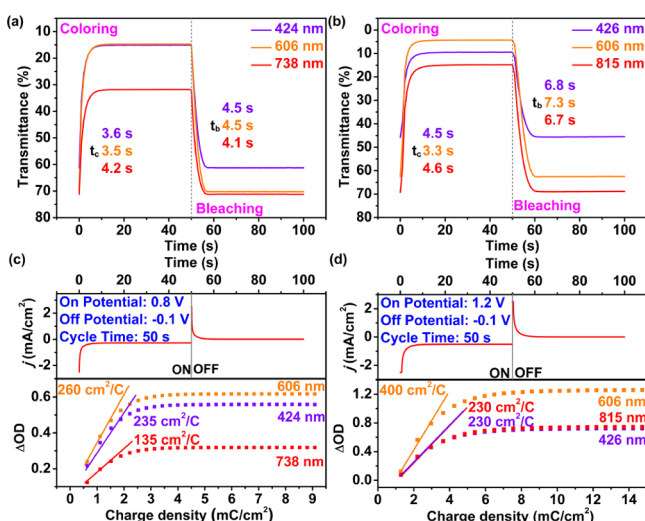


**Figure 8.** EC switching response at the relative wavelength of the EC device derived from (a) NTPPA/HV between 0.8 V (coloring) and  $-0.1 \text{ V}$  (bleaching) and (b) NTPB/HV between 1.0 V (coloring) and  $-0.1 \text{ V}$  (bleaching). Current consumption and change in the in-situ optical density vs the charge density of the ECD based on (c) NTPPA/HV between 0.8 V (coloring) and  $-0.1 \text{ V}$  (bleaching) and (d) NTPB/HV between 1.0 V (coloring) and  $-0.1 \text{ V}$  (bleaching). The device is ITO glass with  $2 \times 2 \text{ cm}^2$  active area containing 0.015/0.015 M NTPPA/HV or NTPB/HV in about 0.05 mL of GBL.

S12. The definition of the switching time is that the time at 90% of the full switched in transmittance as the result of the difficulty for the human eye to perceive any further color change beyond such percentage. As delineated in Figure 8a, the device derived from NTPPA/HV exhibits an average switching time of 3.8 s for the coloring process (0.8 V) and 4.4 s for the bleaching process ( $-0.1 \text{ V}$ ). On the other hand, the device based on NTPB/HV demonstrates an average switching time of 4.2 s for the coloring process (1.0 V) and 6.9 s for the bleaching process ( $-0.1 \text{ V}$ ) as depicted in Figure 8b. In addition, to identify the electrochemical performance of the ECDs, coloration efficiency (CE =  $\Delta\text{OD}/\Delta Q$ ) will be an essential factor. CE describes the change in the optical density ( $\text{OD} = \log(T_b/T_c)$ ) per unit of charge density [ $Q/A$ : amount

of the charge ( $Q$ ) consumed per unit of working area ( $A$ )] throughout the switching process. The changes of optical density at the related absorption wavelength versus injected charge density at the corresponding potentials are plotted in Figure 8c,d. The numerical values of CE could be obtained from the slopes of tangent lines which match with the linear segment of the curves. The average CE of devices from NTPPA/HV is  $210 \text{ cm}^2/\text{C}$  and NTPB/HV is  $287 \text{ cm}^2/\text{C}$ . Furthermore, the EC stability of these devices was also evaluated by measuring the optical absorption change after 1000 switching cycles, confirming excellent stability with only 0.5 and 1.7% decay in transmittance for the devices derived from NTPPA/HV and NTPB/HV, respectively.

#### Electrochemical and EC Behaviors of the EFCDs.

NTPB/HV was further fabricated into an EFCD with a gel-type electrolyte. The electrochemical and EC results of the EFCD shown in Figure 9 reveal the first oxidation potential at

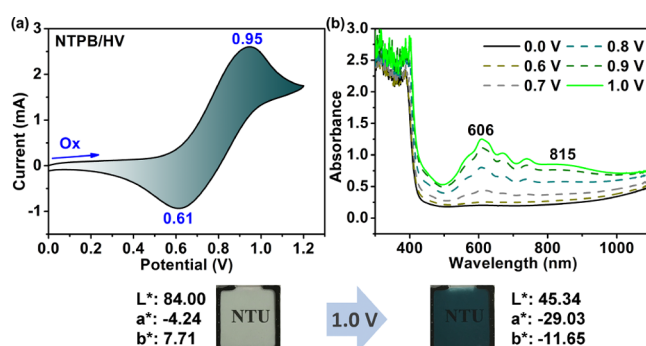


**Figure 9.** (a) Cyclic voltammogram (scan rate: 50 mV/s) and (b) absorbance spectra (applied potential: 0.0–1.0 V) of the electrochromic device (EFCD) derived from NTPB/HV with a gel-type electrolyte. The device is ITO glass with  $2 \times 2 \text{ cm}^2$  active area containing 0.015/0.015 M NTPB/HV in about 0.05 mL of GBL.

0.95 V approximate to those of the ECDs mentioned above. The device demonstrates a color change from the transparent neutral form with  $L^*a^*b^*$  values (84.00,  $-4.24$ , and 7.71) to a blue-green oxidized state with  $L^*a^*b^*$  values (45.34,  $-29.03$ , and  $-11.65$ ) at an applied voltage of 1.0 V.

**EFC Behavior of the EFCD.** The obtained EFCD shows a PL emission maximum ( $\lambda_{em}$ ) at 495 nm, and the fluorescence intensity could be tuned with the applied potentials as shown in Figure 10a,b. Since the applied voltage increased from 0.0 to 1.0 V, the fluorescence of NTPB/HV could be almost extinguished owing to the formation of a NTPB cation radical, resulting in a high PL contrast ratio ( $I_{off}/I_{on}$ ) of 31.21. The EFCD could return to its original fluorescence state after removing the applied potential which means it exhibits electrochemically invertible fluorescence switching behavior between the neutral (fluorescent) state and the oxidized (non-fluorescent) state by a repetitious applied voltage. Figure 10c displays the fluorescence switching time estimated at 90% of the full switching of NTPB/HV which was monitored at 495 nm with 4.9 and 9.7 s for switching on and off, respectively. Besides, the response time-dependent behavior of the PL contrast ratio as depicted in Figure 10d reveals the contrast ratio ranging from 31.21 to 13.49 for the NTPB/HV device when the switching cyclic time was reduced from 360 to 10 s. Furthermore, Figure 11 exhibits long-term stability and reversibility of the EFCD obtained by setting the PL intensity as a function of switching cycles, demonstrating a high

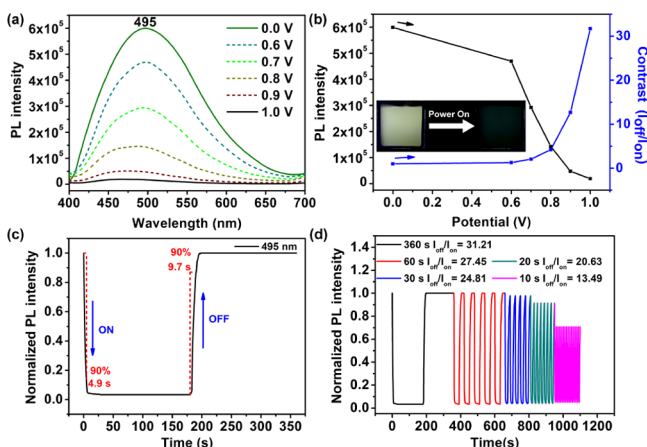


**Figure 10.** (a) PL spectra, (b) potential vs PL and contrast diagram, (c) fluorescence switching responses, and (d) switching time test of a gel-type EFCD derived from NTPB/HV. The switching time test was performed at different step cycle times of 360, 60, 30, 20, and 10 s by applying voltage between  $-0.1$  and  $1.0$  V.

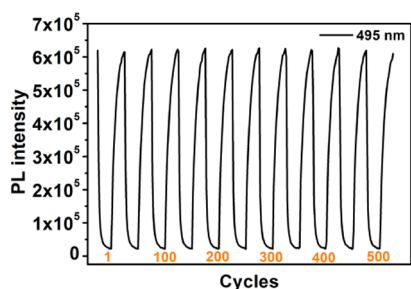


**Figure 11.** Repetitive switching time test of EFCD based on NTPB/HV between  $1.0$  V (on) and  $-0.1$  V (off) with a cycle time of  $15$  s.

reversibility of 99% after 500 cycles for the EFCD derived from NTPB/HV.

## CONCLUSION

Two novel monomeric dimethylamine-containing TPA-based EC materials, NTPPA and NTPB, were readily prepared from Buchwald–Hartwig amination and were further fabricated into ECDs. The dimethylamino substituents not only provide stronger electron-donating ability than the methoxy groups but also multiply the oxidation states comparing to their original structure. The modification can effectively lower their oxidation potential and further reduce the power consumption that makes them more suitable to be utilized as green energy materials. The ECDs derived from these materials accompanying with HV demonstrate good EC stability with a short switching time. Furthermore, NTPB was also confirmed to be a suitable material for the EFC application. The obtained EFC device also demonstrates high PL contrast ratio ( $I_{\text{off}}/I_{\text{on}}$ ), excellent stability, and short switching time, implying great potential of NTPB in optoelectronic applications.

## ASSOCIATED CONTENT

### Supporting Information

The Supporting Information is available free of charge on the ACS Publications website at DOI: 10.1021/acsami.9b00402.

Schematic procedure of gel-type electrofluorochromic device; FT-IR spectra of NDPA and NTPB;  $^1\text{H}$  NMR spectrum of NDPA;  $^{13}\text{C}$  NMR, COSY, and HSQC

spectrum of NTPPA;  $^1\text{H}$  NMR,  $^{13}\text{C}$  NMR, COSY, and HSQC spectrum of NTPPA and NTPB; stability test of the electrochromic devices; crystal data and experimental details, atomic coordinates ( $\times 10^4$ ) and equivalent isotropic displacement parameters ( $\text{\AA}^2 \times 10^3$ ), bond lengths [ $\text{\AA}$ ] and angles [deg], and anisotropic displacement parameters for NTPPA and NTPB; and crystal data and experimental details (PDF)

Crystallographic data (CIF)

Crystallographic data (CIF)

## AUTHOR INFORMATION

### Corresponding Author

\*E-mail: gsliou@ntu.edu.tw.

### ORCID

Guey-Sheng Liou: 0000-0003-3725-3768

### Author Contributions

$\S$ J.-T.W. and H.-T.L. contributed equally.

### Notes

The authors declare no competing financial interest.

## ACKNOWLEDGMENTS

This work was financially supported by the Advanced Research Center of Green Materials Science and Technology from The Featured Area Research Center Program within the framework of the Higher Education Sprout Project by the Ministry of Education (107L9006) and the Ministry of Science and Technology in Taiwan (107-3017-F-002-001 and 107-2113-M-002-024-MY3).

## REFERENCES

- Platt, J. R. Electrochromism, a Possible Change of Color Producing in Dyes by an Electric Field. *J. Chem. Phys.* **1961**, *34*, 862–863.
- Azens, A.; Granqvist, C. Electrochromic Smart Windows: Energy Efficiency and Device Aspects. *J. Solid State Electrochem.* **2003**, *7*, 64–68.
- Yang, P.; Sun, P.; Mai, W. Electrochromic Energy Storage Devices. *Mater. Today* **2016**, *19*, 394–402.
- Wang, Y.; Runnerstrom, E. L.; Milliron, D. J. Switchable Materials for Smart Windows. *Annu. Rev. Chem. Biomol. Eng.* **2016**, *7*, 283–304.
- Dautremont-Smith, W. C. Transition metal oxide electrochromic materials and displays: a review. *Displays* **1982**, *3*, 3–22.
- DeLongchamp, D. M.; Hammond, P. T. High-Contrast Electrochromism and Controllable Dissolution of Assembled Prussian Blue/Polymer Nanocomposites. *Adv. Funct. Mater.* **2004**, *14*, 224–232.
- Weng, D.; Shi, Y.; Zheng, J.; Xu, C. High Performance Black-to-Transmissive Electrochromic Device with Panchromatic Absorption Based on TiO<sub>2</sub>-Supported Viologen and Triphenylamine Derivatives. *Org. Electron.* **2016**, *34*, 139–145.
- Beaujuge, P. M.; Reynolds, J. R. Color Control in  $\pi$ -Conjugated Organic Polymers for Use in Electrochromic Devices. *Chem. Rev.* **2010**, *110*, 268–320.
- Neo, W. T.; Ye, Q.; Chua, S.-J.; Xu, J. Conjugated Polymer-Based Electrochromics: Materials, Device Fabrication and Application Prospects. *J. Mater. Chem. C* **2016**, *4*, 7364–7376.
- Huang, D.-C.; Wu, J.-T.; Fan, Y.-Z.; Liou, G.-S. Preparation and Optoelectronic Behaviours of Novel Electrochromic Devices Based on Triphenylamine-Containing Ambipolar Materials. *J. Mater. Chem. C* **2017**, *5*, 9370–9375.
- Laschuk, N. O.; Ebraldzde, I. I.; Poisson, J.; Egan, J. G.; Quaranta, S.; Allan, J. T. S.; Cusden, H.; Gaspari, F.; Naumkin, F. Y.; Easton, E. B.; Zenkina, O. V. Ligand Impact on Monolayer

Electrochromic Material Properties. *ACS Appl. Mater. Interfaces* **2018**, *10*, 35334–35343.

(12) Deb, S. K. A Novel Electrophotographic System. *Appl. Opt.* **1969**, *8*, 192–195.

(13) Nguyen, W. H.; Barile, C. J.; McGehee, M. D. Small Molecule Anchored to Mesoporous ITO for High-Contrast Black Electrochromics. *J. Phys. Chem. C* **2016**, *120*, 26336–26341.

(14) Resch-Genger, U.; Hennrich, G. Fluorescent Redox-Switchable Devices. *Top. Fluoresc. Spectrosc.* **2005**, *9*, 189–218.

(15) Rusalov, M. V.; Druzhinin, S. I.; Uzhinov, B. M. Intramolecular Fluorescence Quenching of Crowned 7-Aminocoumarins as Potential Fluorescent Chemosensors. *J. Fluoresc.* **2004**, *14*, 193–202.

(16) Kim, Y.; Kim, E.; Clavier, G.; Audebert, P. New Tetrazine-Based Fluoro-electrochromic Window; Modulation of the Fluorescence Through Applied Potential. *Chem. Commun.* **2006**, *0*, 3612–3614.

(17) Kuo, C.-P.; Chuang, C.-N.; Chang, C.-L.; Leung, M.-k.; Lian, H.-Y.; Chia-Wen Wu, K. White-Light Electrofluorescence Switching from Electrochemically Convertible Yellow and Blue Fluorescent Conjugated Polymers. *J. Mater. Chem. C* **2013**, *1*, 2121–2130.

(18) Wu, J.-H.; Liou, G.-S. High-Performance Electrofluorochromic Devices Based on Electrochromism and Photoluminescence-Active Novel Poly(4-Cyanotriphenylamine). *Adv. Funct. Mater.* **2014**, *24*, 6422–6429.

(19) Beneduci, A.; Cospito, S.; Deda, M. L.; Chidichimo, G. Highly Fluorescent Thienoviologen-Based Polymer Gels for Single Layer Electrofluorochromic Devices. *Adv. Funct. Mater.* **2015**, *25*, 1240–1247.

(20) Xing, H.; Zhang, X.; Zhai, Q.; Li, J.; Wang, E. Bipolar Electrode Based Reversible Fluorescence Switch Using Prussian Blue/Au Nanoclusters Nanocomposite Film. *Anal. Chem.* **2017**, *89*, 3867–3872.

(21) Liu, J.; Shi, Y.; Wu, J.; Li, M.; Zheng, J.; Xu, C. Yellow Electrochromic Polymer Materials With Fine Tuning Electrofluorescences by Adjusting Steric Hindrance of Side Chains. *RSC Adv.* **2017**, *7*, 25444–25449.

(22) Santra, D. C.; Nad, S.; Malik, S. Electrochemical Polymerization of Triphenylamine End-Capped Dendron: Electrochromic and Electrofluorochromic Switching Behaviors. *J. Electroanal. Chem.* **2018**, *823*, 203–212.

(23) Cheng, S.-W.; Han, T.; Huang, T.-Y.; Tang, B.-Z.; Liou, G.-S. High-Performance Electrofluorochromic Devices Based on Aromatic Polyamides With AIE-Active Tetraphenylethene and Electro-Active Triphenylamine Moieties. *Polym. Chem.* **2018**, *9*, 4364–4373.

(24) Thelakkat, M. Star-Shaped, Dendrimeric and Polymeric Triarylamines as Photoconductors and Hole Transport Materials for Electro-Optical Applications. *Macromol. Mater. Eng.* **2002**, *287*, 442–461.

(25) Yen, H.-J.; Liou, G.-S. Solution-Processable Triarylamine-Based Electroactive High Performance Polymers for Anodically Electrochromic Applications. *Polym. Chem.* **2012**, *3*, 255–264.

(26) Yen, H.-J.; Liou, G.-S. Recent Advances in Triphenylamine-Based Electrochromic Derivatives and Polymers. *Polym. Chem.* **2018**, *9*, 3001–3018.

(27) Liu, H.-S.; Pan, B.-C.; Huang, D.-C.; Kung, Y.-R.; Leu, C.-M.; Liou, G.-S. Highly Transparent to Truly Black Electrochromic Devices Based on an Ambipolar System of Polyamides and Viologen. *NPG Asia Mater.* **2017**, *9*, No. e388.

(28) Jennings, J. R.; Lim, W. Y.; Zakeeruddin, S. M.; Grätzel, M.; Wang, Q. A Redox-Flow Electrochromic Window. *ACS Appl. Mater. Interfaces* **2015**, *7*, 2827–2832.

(29) Wu, J.-T.; Liou, G.-S. A Novel Panchromatic Shutter Based on an Ambipolar Electrochromic System without Supporting Electrolyte. *Chem. Commun.* **2018**, *54*, 2619–2622.

(30) Leventis, N.; Chen, M. G.; Liapis, A. I.; Johnson, J. W.; Jain, A. Characterization of  $3 \times 3$  Matrix Arrays of Solution-Phase Electrochromic Cells. *J. Electrochem. Soc.* **1998**, *145*, L55–L58.

(31) Ho, K.; Fang, Y. W.; Hsu, Y. C.; Chen, L. C. The Influences of Operating Voltage and Cell Gap on the Performance of a Solution-

Phase Electrochromic Device Containing HV and TMPD. *Solid State Ionics* **2003**, *165*, 279–287.

(32) Hsiao, S.-H.; Liou, G.-S.; Kung, Y.-C.; Yen, H.-J. High Contrast Ratio and Rapid Switching Electrochromic Polymeric Films Based on 4-(Dimethylamino)triphenylamine-Functionalized Aromatic Polyamides. *Macromolecules* **2008**, *41*, 2800–2808.